Biosensors and Bioelectronics 89 (2017) 773–780

Contents lists available at ScienceDirect

Biosensors and Bioelectronics

journal homepage: www.elsevier.com/locate/bios

Amplified fluorescent sensing of DNA using luminescent carbon dots and AuNPs/GO as a sensing platform: A novel coupling of FRET and DNA hybridization for homogeneous HIV-1 gene detection at femtomolar level

Somaye Hamd Qaddare[a], Abdollah Salimi[a,b,*]

[a] Department of Chemistry, University of Kurdistan, 66177-15175, Sanandaj, Iran
[b] Research Center for Nanotechnology, University of Kurdistan, 66177-15175, Sanandaj, Iran

ARTICLE INFO

Keywords:
DNA hybridization
Carbon dot
Fluorescence resonance energy transfer
HIV-1 gene
Gold nanoparticles
Graphene oxide

ABSTRACT

The demand for simple, sensitive, affordable, and selective DNA biosensors is willing, due to the important role of DNA detection in the areas of disease diagnostics, environment monitoring and food safety. The presented work is devoted to the fabrication of an ultrasensitive homogeneous biosensor for the detection of DNA sequences related to HIV based on fluorescence resonance energy transfer(FRET) between carbon dots(CDs) and AuNPs as nanoquenchers. CDs as fluorophore with average size 3–4 nm were prepared by hydrothermal treatment of histidine. In this respect, the hybridization was occurring between the assemblies of fluorescence CDs functionalized 5-amino-labeled oligonucleotides as capture probe and label free oligonucleotides as detection probe. Due to strong fluorescence and good biocompatibility of CDs, the capture probe was covalently conjugated to CDs. In the presence of the target probe, the association between capture probe-CDs and detection probe is stronger than that between capture probe-CDs and AuNPs, leading to the release of the capture probe-CDs from AuNPs, resulting in the recovery of the fluorescence of CDs. This oligonucleotides detection probe was observed to detect target oligonucleotides specifically and sensitively in a linear range from 50.0 fM to 1.0 nM with a detection limit of 15 fM. Furthermore, the sensitivity of this FRET strategy amplified using AuNPs/graphene oxide nanocomposite as quencher. The Sensor response indicates only the complementary sequence showing an obvious change signal in comparison to non-complementary and two bases mismatched sequences. Moreover, satisfactory results from determination of HIV DNA target in human serum were obtained showing great potential of the proposed method for real sample analysis. The proposed biosensor with highly biocompatibility and nontoxicity, can be developed for detection of other DNA biomarkers.

1. Introduction

Biomolecular detection has become more and more critical in early diagnostics and treatment of diseases, thereby prompting intensive interest in the development of trustworthy, simple and low-cost biosensors for proteins, nucleic acids and other biomolecules (Bohunicky and Mousa, 2011; Tothill, 2009). Acquired Immunodeficiency Syndrome (AIDS) occurs when infection with the Human Immunodeficiency Virus (HIV) destroys the body's natural protection from illness. The HIV/AIDS pandemic has killed 39 million people worldwide, and nearly as many people are living with HIV infection today. Up to now, several techniques including single strand conformation (Taylor and Taylor, 2004), high performance liquid chromatography (Choi et al., 2007), real-time PCR (Pau et al., 2010), optical (Shafiee et al., 2014), and electrochemical (Ruan et al., 2014) transducers, in the areas of medicinal diagnosis and biochemical analysis for the detection of HIV have been reported. However, these methods still have some limitations as they are complex, time consuming and expensive. Some serologic tests as standard HIV assays, including the enzyme-linked immunosorbent assay (ELISA) and Western blot assay are very sensitive, the ELISA suffers the shortcomings of false positive and false negative results and Western blot assay might be indeterminate or falsely negative if a blood specimen is collected at the time too closed to the infection (Proffitt, 1993). Therefore, there is a clear need for researchers to develop sensitive and specific analytical and diagnostic techniques that detect HIV at the earliest possible time following infection. Thus, researchers are interested in developing a direct nucleic acid- based test which can detect the presence of DNA sequences related to HIV (Lee et al., 2004). Recently, novel nanomaterials have attracted great attention in biolo-

* Corresponding author at: Department of Chemistry, University of Kurdistan, 66177-15175, Sanandaj, Iran.
E-mail addresses: absalimi@uok.ac.ir, absalimi@yahoo.com (A. Salimi).

http://dx.doi.org/10.1016/j.bios.2016.10.033
Received 27 August 2016; Received in revised form 7 October 2016; Accepted 18 October 2016
Available online 19 October 2016
0956-5663/

gical analysis and detection (Gedi and Kim, 2014; Chikkaveeraiah et al., 2012). Recently, we used different semiconductor materials such as CdS, CdTe, TiO_2 for the detection of biological species such as NADH, glucose and also measuring of hydrogen peroxide and ethanol (Jafari et al., 2014a, 2014b, Salimi et al., 2013, Navaee and Salimi, 2013, Arabzadeh et al., 2016). Carbon dots (CDs), a new class of quasi-spherical fluorescent nanomaterials, have attracted much attention in recent years (Lim et al., 2015). Compared to the conventional semiconductor quantum dots (QDs) and organic fluorescent dyes, CDs possess numerously superior features including easy preparation and functionalization, no/low toxicity and high photostability, thus demonstrating a variety of potential applications, such as sensing, biomedicine, catalysis, and optoelectronic devices (Zhang et al., 2015). Graphene, a two-dimensional aromatic sheets of sp^2-bonded carbon atoms with large specific surface area, excellent electrical and thermal conductivity, good biocompatibility, strong mechanical strength, and low manufacturing cost is an interesting substrate for the immobilization of inorganic nanoparticles (Muszynski et al., 2008). The integration of two-dimensional GO with zero-dimensional AuNPs produce a AuNPs/GO nanohybride that not only combine the characteristics of each component, but possess interesting structural, electrochemical, electromagnetic, and other properties that are not available in their respective components.

Recently, sequence-specific DNA detection has received more and more attentions due to its extreme importance in clinical molecular diagnostics of diseases, biomedical studies, microbiology, and genetics (Song et al., 2008). Among electrochemical, optical and gravimetric methods for DNA detection, fluorescence-based assay offers various advantages such as high sensitivity, easy to operate and multiplexing capabilities. The fluorescent resonant energy transfer (FRET) is one of the most popular strategies in fluorescence based assays, which can provide high sensitivity and selectivity toward the target (Chen et al., 2012). The FRET process occurs when (i) the emission spectra of the fluorophore (energy donor) overlap with the absorption of the quencher (energy acceptor) and (ii) the energy donor and acceptor are close to each other, typically within 10 nm. The energy donor should provide a stable fluorescent output, highly resistant to photobleaching, and the acceptor should possess high absorptivity. Meanwhile, the FRET process need to be selectively responsive to the desired target, thus the corresponding change in fluorescence intensity can be used to quantify the target concentration.

Taking advantage of the unique optical properties of CDs, AuNPs, and AuNPs/GO composite, here, we report a simple sensing platform for HIV DNA sequence determination with a FRET strategy. The obtained CDs with carboxyl groups can easily load DNA through covalence bond by activating through EDC/NHS. CDs and AuNPs were first connected with each other, which lead to the quench of the luminescence. Upon the present of the target (HIV DNA), CDs will leave the surface of AuNPs and the luminescence can be restored due to the formation of the more stable double-stranded DNA(dsDNA) on CDs. Then to evaluate the sensitivity and the role of components, AuNPs as the quenchers in this fabricated biosensor were composed with graphene oxide. Accordingly, the amount of received enhanced fluorescence response showed the amplified sensitivity of this FRET strategy, using AuNPs/GO nanocomposite as quencher. Here in reversible donor quenched mode FRET, the quenched fluorescence of CDs turns “on” again after the release of AuNPs/GO from the surface. This DNA hybridization system with release process based on highly fluorescent and biocompatible CDs holds great promise for DNA hybridization studies. Once you had known the optimal conditions, the utility of the new optical hybridization indicator could provide a simple, rapid detection and might have a promising future in transducing DNA hybridization. It was showed that the method developed in this work has high selectivity and sensitivity for DNA detection related to HIV gene at femtomolar concentration range, while very low responses observed for non-complementary oligonucleotides and two bases mismatch.

2. Experimental section

2.1. Materials and instruments

All starting materials were obtained from commercial suppliers. Tetrachloroauric acid ($HAuCl_4$) and all other reagents with analytical grade were from Merck or Fluka. 1-Ethyl-3-(3-dimethylaminopropyl) carbodiimide hydrochloride (EDC), N-hydroxysuccinimide (NHS), were purchased from Abcam Company (Cambridge, UK). Dialysis bags (molecular weight cut off =1000 Da) were also ordered from Sigma-Aldrich. The HIV related DNA strands were synthesized by BIONEER, Global Genomics Partner and purified using HPLC. Their sequences were as follows:

HIV probe: 5-NH_2-GGGGGGCCAAGGCCCAGCCCTCACACA.

Complementary strand (cDNA):5-TGTGTGAGGGCTGGGCCTTGG-3.

A two-base mismatched strand (mDNA) was as follows: TGTCTGAGGGCTCGGCCTTGG.

Non-complementary-strand (nDNA): GGTTCCGGGTCGGGAGTGTGT.

The instruments applied for absorption, fluorescence emission and material characterization are reported in SI file.

2.2. Synthesis of carbon dots (CDs)

CDs were synthesized according to previous typical literature (Dai et al., 2014). Fluorescent CDs were prepared by hydrothermal treatment of histidine. Typically in the first step, 2.5 g histidine was dissolved in 25 mL NaOH (0.5 mol L^{-1}) solution and then transferred into a 50-mL Teflon-lined autoclave and heated at 180 °C for a period of 12 h. The CDs were collected by removing the large dots through centrifugation. Then the carbogenic nanoparticles obtained above were dialyzed against Milli-Q water for 2 days through a dialysis membrane to remove the excess precursors and resulting small molecules. The suspension appeared homogeneous light yellow and was stored at 4 °C in a refrigerator.

2.3. Synthesis of AuNPs and AuNP/GO conjugates

The synthesis of AuNPs and AuNP/GO conjugates described in SI file. Briefly, AuNPs were prepared by the citrate reduction of $HAuCl_4$ using the method according to the literature and Cysteamine capped AuNPs were synthesized via chemical reduction of gold chloride solution (Lee et al., 2008). The obtained cysteamine-AuNP solution (5 mL) was then mixed with GO solution (5 mL at 2 mg/mL), followed by addition of 40 mg ethyl (dimethylaminopropyl) carbodiimide (EDC) with shaking for 10 h (details reported in SI).

2.4. Attachment of HIV probe to CDs

The HIV probe covalently attached to carbon dots using EDC/NHS as activating agents. Briefly, NHS and EDC solution (1 mmol/mL, 1 mL) were added to 1 mL of the clear carboxylate-modified CD solution. Then these activated CDs were centrifuged and after that 1 mL of HIV DNA capture probe was added to this mixture and the prepared CDs-DNA probe storing in the refrigerator at 4 °C.

3. Results and discussion

3.1. Morphological and spectral characterizations of AuNPs, AuNPs/GO and CDs

The size and morphology of the CDs were characterized by TEM. It can be seen that the as-synthesized CDs were uniform in size and

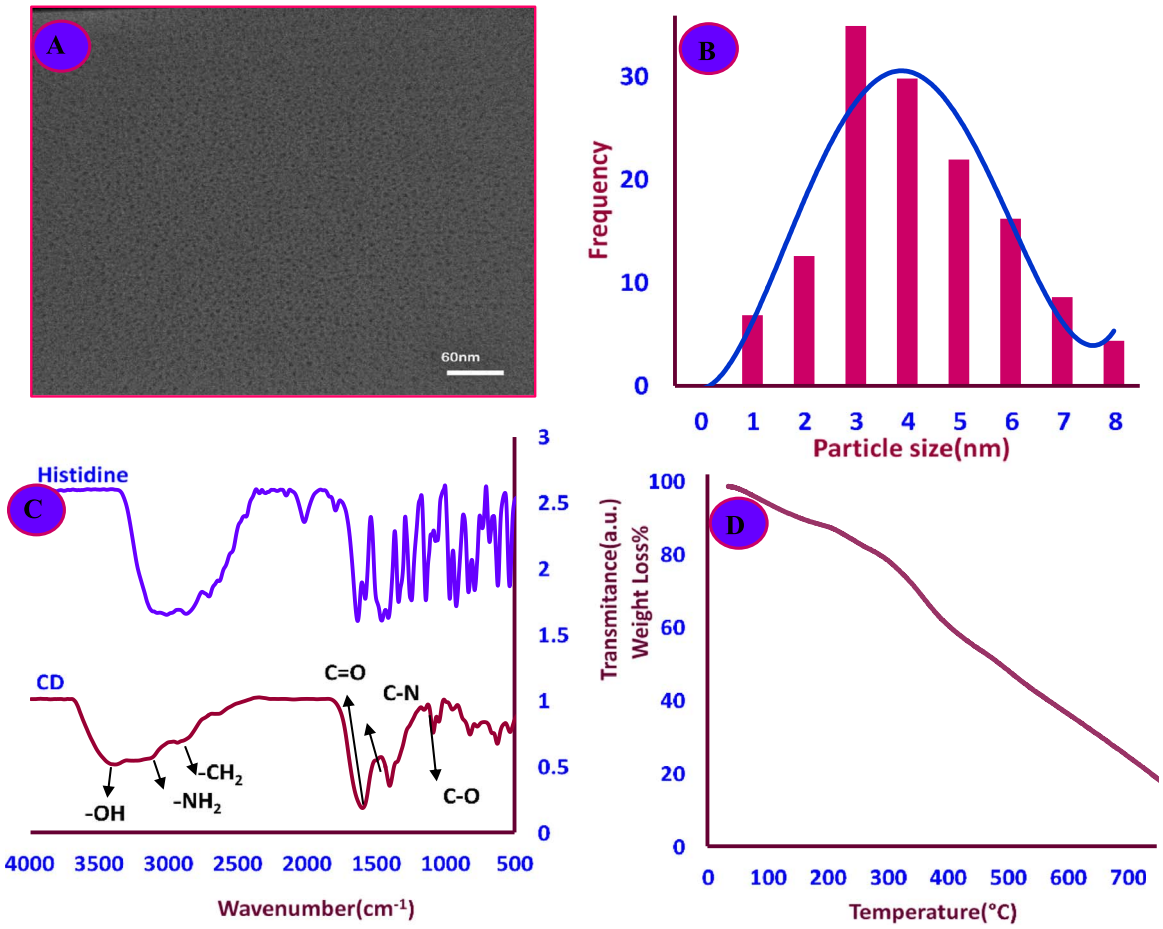

Fig. 1. (A) HRTEM image and (B) TEM histogram and Gauss fitting of particle size distribution of CDs. (C) FTIR spectrum and (D) TGA spectrum of CDs..

possess a nearly spherical shape with a diameter of ca. 3–4 nm (Fig. 1A and B). The FTIR results of the obtained CDs (Fig. 1C) and synthesized AuNP/GO composite (Fig. S1) with characteristic wavenumbers, indicated the successful synthesis of proposed nanostructures. Fig. 1D shows the TGA spectrum of CDs, the resulted loss of weight at different temperatures indicates the thermal stability of the structure. The details of the thermal analysis is reported in SI. Fig. 2A illustrated the typical absorption, excitation and emission of the obtained CDs. In Fig. 2B, the fluorescence spectra displayed that the maximum emission wavelength moved to a longer wavelength with an increased intensity as the excitation wavelength increased and the emission peak position shifts to longer wavelengths, then the intensity gradually decreases. The fluorescent intensity reached the highest value when excited at 350 nm. This excitation-dependent emission individuality was widely observed in various luminescent carbon nanomaterials, which might be caused by the optical selection of different surface defect states near the fermi level of CDs (Tang et al., 2012). Fig. 2C shows the normalized PL emission spectra of the CDs with different excitation wavelengths from 280 to 410 nm. It can be seen that the emission spectrum of the changes from 420 nm to 500 nm. The emission peak position shifts to longer wavelengths as the excitation wavelength increases. The maximum fluorescence emission intensity can be obtained when it is excited at 350 nm. From the basic to occur the FRET is the existing of appreciable overlap between the emission spectrum of the donor and the absorption spectrum of the acceptor. As can be seen in Fig. 2D the UV–vis absorption of AuNPs (centered at 520 nm) and AuNPs/GO (centered at 535 nm) have good overlap with the fluorescence emission band of CDs (centered at 460 nm), suggesting that an efficient energy transfer between them can take place. In Fig. 2E the UV–vis absorption of the prepared CDs, ss DNA, ss DNA-CDs, and ss DNA-CDs-AuNPs are displayed. The CDs shows abroad absorption peak centered at 308 nm, which is possibly due to the relatively broad size distribution of CDs (Li et al., 2014). The absorption edge that is extended to 400 nm was only found in CDs (specific details in SI), indicating the formation of CDs (Jaiswal et al., 2012). The UV–vis absorption spectrum of AuNPs, GO, and AuNPs/GO, are shown in Fig. 2F and as illustrated, the changes in UV–vis absorption spectra of AuNPs and GO species showed that the AuNPs decorated onto GO successfully. In addition, the AFM (A) and size distribution (B) image of CDs is shown in Fig. S2. The direct evidence of the formation of gold nanoparticles on the planes and edges of graphene sheets and morphologies of the decorated dispersed nanoparticles was also characterized by taking SEM image (Fig. S3). As can be seen gold nanoparticles with diameter 5–30 nm uniformly decorated onto graphene nanosheets. In Fig. S4(A) a digital photo related of AuNPs, GO and AuNPs/GO composite is shown and the color changes for synthesized AuNPs/GO composite indicated.

3.2. Probe immobilization

3.2.1. Activating CDs using EDC/NHS coupling

Herein, fabrication of an optical biosensor by using coupling of the DNA-conjugated CDs- AuNPs and DNA-conjugated CDs-AuNPs/GO for highly sensitive detection of DNA activity to the construction of a FRET DNA hybridization system was proposed. For both strategies of hybridization and FRET, the designed single-stranded DNA (ss-DNA) has amino groups, at one ends, which could be conjugate with CDs carboxyl group through covalent binding. The color changes of capture probe ssDNA-CDs (a), capture probe ssDNA-CDs-AuNPs (b), and capture probe ssDNA-CDs-AuNPs in the present of target DNA

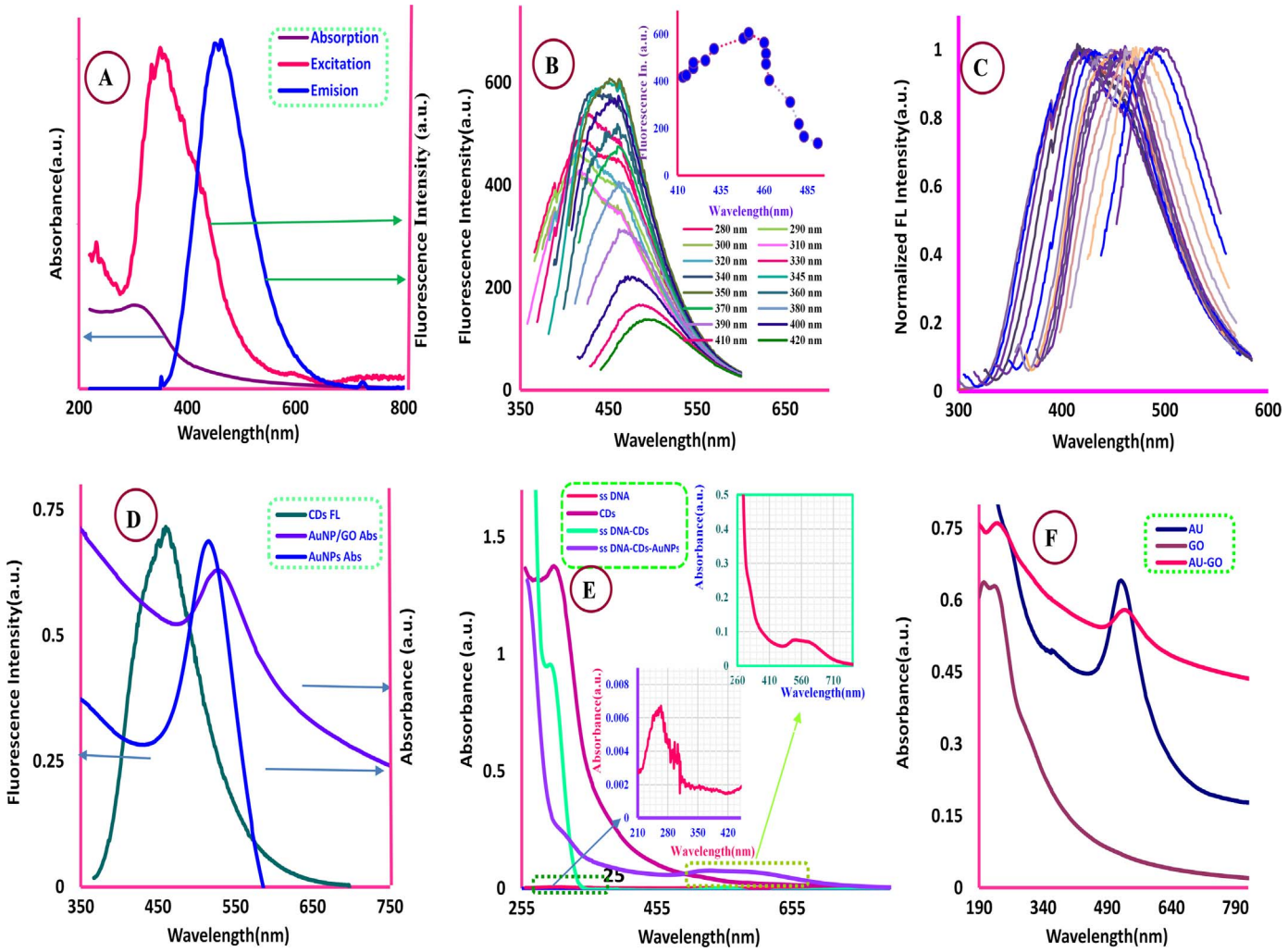

Fig. 2. (A) illustrated the typical absorption, excitation and emission of the obtained CDs. (B) Fluorescent spectra of diluted aqueous solution of CDs at different excitation wavelengths from left to right: (progressively longer excitation wavelengths from 280 nm to 420 nm with a 10 nm increment), (C) Normalized fluorescent spectra of CDs, (D) overlapping of emission of CDs and absorption spectra of AuNPs and AuNP/GO. (E) displayed the UV–vis absorption spectrum of ss capture probe DNA, CDs, ss capture probe DNA-CDs, ss capture probe DNA-CDs-AuNPs. The UV–vis absorption spectra of AuNPs, GO and AuNPs/GO..

(cDNA) is shown in Fig. S4B. Although we have to mention here that the proposed strategy was tested at first by using the amine group of the probe DNA and amine group on the surface of the as-prepared CD, to be conjugated using glutaraldehyde as linker, but this kind of conjugation lead to a change in the peak shape and peak position of the CDs (Fig. S5). So the fabrication processes were conducted using carboxyl group. The immobilization of the DNA probes was confirmed using fluorescence spectra (Fig. S6). The covalence binding between CDs and capture probe ssDNA in the presence of activating agent increasing the rigidity of fluorophore structures and finally enhancement of the fluorescence response.

3.2.2. Fluorescence quenching of CDs by AuNPs and AuNPs/GO

In this FRET sensing system, we employed nanomaterials such as CDs as the donor and AuNPs and AuNPs/GO as the fluorescence acceptors (quencher). To fabricate an effective biosensor, there are several key factors that influencing the performance of DNA hybridization FRET sensing system. One of them is to find suitable nanomaterials such as carbon based nanostructures with high activity sites to immobilize signal probes. Furthermore, the role of gold nanoparticles in biological systems is so important because of their high extinction coefficient, conjugation of these particles to the biomolecules, broad absorption spectrum in a visible light that is overlapped with the emission wavelength of common energy donors and their tunable optical properties. Nowadays GO due to its large surface area and unique electronic, thermal, mechanical, and chemical properties attracted great attention. AuNPs decorated onto graphene sheets can be used as supporting material. Deposition of AuNPs onto GO has been demonstrated to reveal special features in new hybrids that can be widely utilized in sensors or biosensors fabrication. This AuNPs/GO nanocomposites exhibited high optical activities towards the fluorescence quenching of CDs by significantly decreasing their fluorescence in several minutes compared with AuNPs. The proposed optical sensor by using AuNPs/GO nanocomposites as a great candidate material showed excellent selectivity and high sensitivity because of its unique structure and properties. It can be seen (Fig. 2D) that obviously the emission spectrum of CDs could overlap well with the absorption spectrum of AuNPs and AuNPs/GO, indicating the potential to produce efficient energy transfer. By injection of amino-functionalized CDs (Fig. S4(B)) into the AuNPs and AuNPs/GO solution, this functionalized CDs can be adsorbed onto the surface of citrate-stabilized AuNPs that is clear by changing the color that turned from red wine to gray- purple. But it is clearly observed that the CDs -AuNPs and CDs-AuNPs/GO conjugates are well dispersed, and the electrostatic interaction is not strong enough to change the suspension state of AuNPs. As shown in Fig. S7A and S7B, the fluorescence intensity of CDs-AuNPs and CDs-AuNPs/GO assemblies is proportional to the concentration of AuNPs and AuNPs/GO. Since, the fluorescence intensity more quenched when

AuNPs/GO was used as quencher compared to AuNPs, so, for increasing the sensitivity of the method we used AuNPs/GO as quencher for measurement experiments.

3.3. Sensing mechanism

The DNA hybridization experiment was carried out at the room temperature. The fluorescence detection was performed at excitation and emission wavelengths of 350 nm and 461 nm, respectively. The AuNPs include a metallic core surrounded by a citrate groups, when CD-ssDNA was added to the AuNPs or AuNPs/GO suspension, CDs in contact with probe DNA was closed to the surface of the AuNPs from their NH_2 groups, and –ssDNA-CD/AuNPs, –ssDNA-CD/ AuNPs/GO assemblies were formed. When the target DNA sequences (cDNA) was added into the system, by the formation of the CD-ssDNA/cDNA duplex and so an assembly with more negative charge density in contrast to CD-ssDNA, stronger electrostatic repulsion between the CD-ssDNA/cDNA duplex (dsDNA) and AuNPs will give arise. The hydrogen bonds between complementary bases are a fundamental feature of the double helix, contributing to the thermodynamic stability of the helix and providing the information content and specificity of base pairing. The, second important contribution comes from stacking interactions between the bases. The bases are flat, relatively water insoluble molecules, and they tend to stack above each other roughly perpendicular to the direction of the helical axis. Furthermore, electron cloud interactions between bases in the helical stacks contribute significantly to the stability of the double helix. Consequently, the distance between the CD units, AuNPs and AuNPs/GO is increased, which gives rise to decrease efficient FRET from the CD to the AuNPs and AuNPs/GO and, the quenched fluorescence of CDs turns “on” again after the release of AuNPs or AuNPs/GO from the surface.(scheme 1)

As discussed in earlier section the formation of CDs-AuNPs is characterized by UV–vis absorption spectrum a broad absorption peak at about 520 nm which is characteristic of AuNPs was displayed in Fig. 2D and E. Also, the fluorescence spectrum of CDs-AuNPs further confirmed the formation of CDs-AuNPs complex, which has an apparent quenching of fluorescence intensity than CDs as illustrated in Fig. S7 A. This is possibly because the AuNPs had a larger superficial area, with increasing of AuNPs concentration, the absorption capacity to CDs became higher, which lead to the fluorescence of CDs be more heavily quenched. In the presence of target DNA sequences, the ssDNA probe switched its structure and the NPs dissociated. As a result, purple-colored aggregates separated into red-colored individual NPs Fig. 3A (inset). This assay format can be used to analyze a broad range of molecules by simple replacement of the DNA sequences. Upon binding of the target, the DNA strands underwent a structure-switching event that led to their dissociation from AuNPs.

3.4. Optimized condition for the target DNA detection

Considering that the assay conditions, such as the ratio of CDs, AuNPs and AuNPs/GO, incubation temperature, and time, have a significant effect on the detection of target DNA sequence, so these conditions were optimized for better sensing performances. It is also important to select the appropriate concentration of CDs, the AuNPs, and AuNPs/GO. The optimized concentrations of CDs, AuNPs and AuNPs/GO were 50 μg/mL, 0.22 nM and 5 μg/mL respectively, which would give out remarkable quenching efficiency (75%) to CDs when the sensor was quenched by AuNPs (Fig. S7A) and reached to 95% when the quencher is replaced by AuNPs/GO (Fig. S7B). A suitable incubation time of capture probe ssDNA-CD and AuNPs is expected to yield a satisfied detection result. As shown in Fig. S8, 5 min of incubation time was enough for the both of systems to reach the equilibrium. To

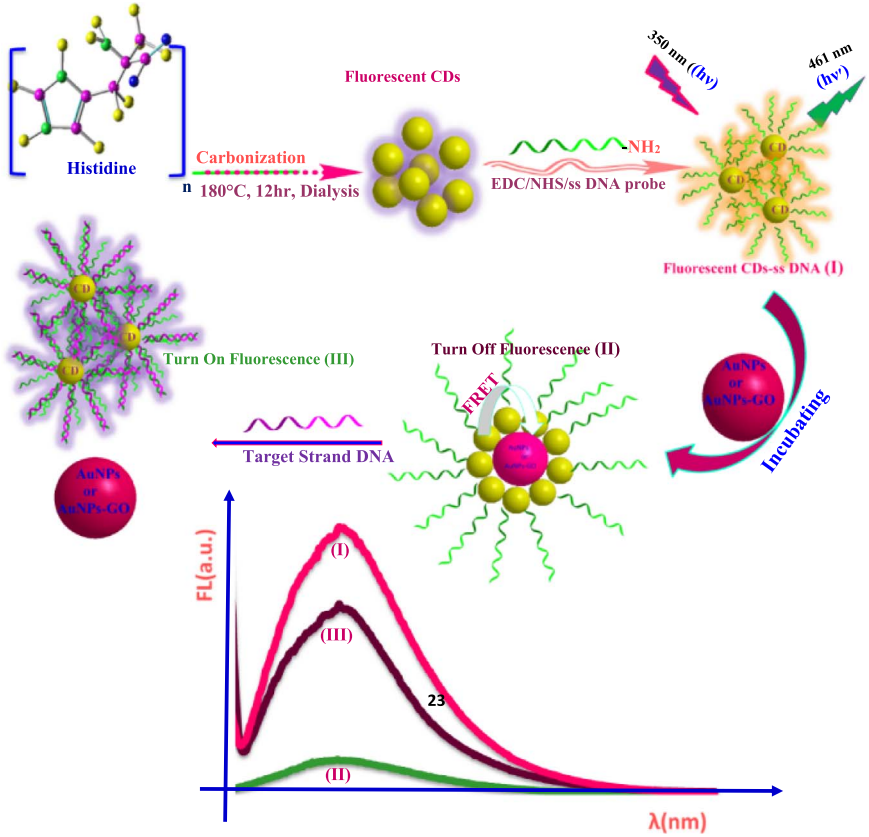

Scheme 1. The mechanism for the FRET-based detection system: in the first part the fluorescence of ss DNA- CDs was quenched by AuNPs/AuNPS-GO through FRET; and then the fluorescence of CDs was recovered in the presence of target DNA.

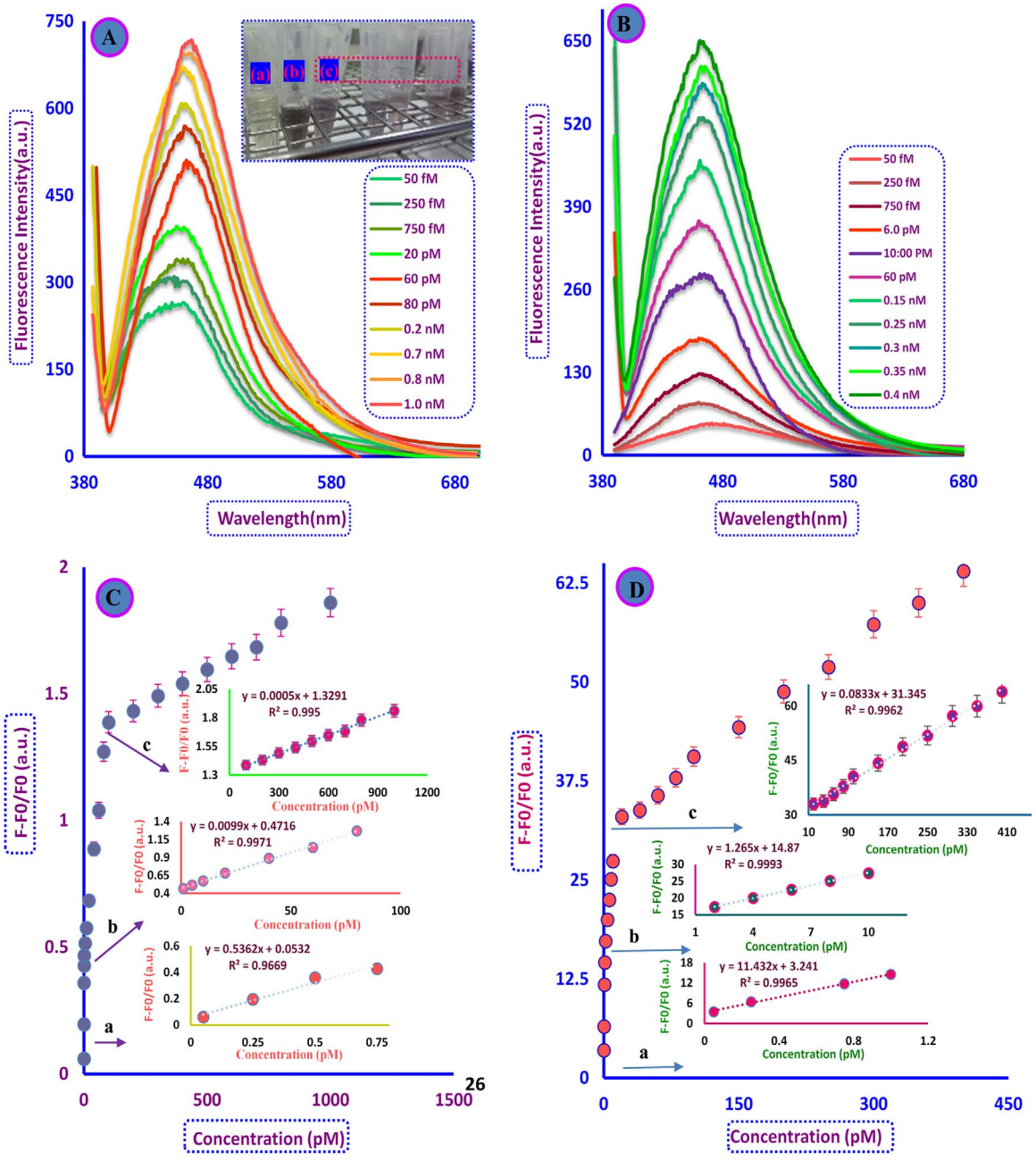

Fig. 3. (A) Fluorescence recovery spectra of the capture probe ssDNA-CDs/AuNPs system in the presence of different concentrations of target DNA at the excitation wavelength of 350 nm and 0.22 nM of AuNPs as quencher, (Inset; digital image of ss DNA-CDs (labeled a vials), ss DNA-CDs-AuNPs (labeled b vials), and ss capture probe DNA-CDs-AuNPs in presence different target DNA concentration (labeled c vials). (B) The fluorescence recovery spectra of the ssDNA-CDs-AuNPs/GO in the presence of different concentrations of target DNA at excitation wavelength of 350 nm and 5 μg/mL of GO/AuNPs as quencher. (C) and 3(D) shows the linear relationship of fluorescence intensity of ss DNA-CDs-AuNPs, ss DNA-CDs-AuNPs/GO complex with different target DNA concentrations..

determine the applicability of this strategy, the fluorescence response of this anti-aggregation assay system under different conditions was measured. As illustrated in Fig. S7 B, the initial fluorescence of CDs was greatly quenched in the presence of 5 μg/mL AuNPs/GO. Furthermore, in the presence of cDNA and DNA- hybridization, no FRET signal from CDs to AuNPs/GO was observed (Fig. 3B), indicate that CDs cannot bind with AuNPs adsorbed on GO surface. This may be attributed to the high binding affinity between ss-DNA capture probe and cDNA. When ssDNA-CDs hybridized with its target DNA, strong FRET signal disrupted, following a red-shift of the emission from 461 to 468 nm. The enhanced fluorescence and the red-shift are due to the formation of dsDNA during DNA hybridization, which separates CDs from AuNPs/GO surface and makes it close.

3.5. HIV-1 target analysis

The quantitative behavior of the DNA biosensor was assessed by measuring the dependence of fluorescence response on the concentration of the HIV-1 gene under optimized conditions. Fig. 3A and B shows fluorescence spectra for the biosensor with different concentrations of the target DNA. Furthermore the variations of fluorescence signal verses target DNA concentration recorded in Fig. 3C and D and a good linear relationship between increased PL intensity (461 nm) and increasing of target DNA concentration was observed. Furthermore, as illustrated the change in fluorescence response is higher when AuNPs/GO used as quencher compared to AuNPs and about 95% of fluorescence signal was quenched by AuNPs/GO (Fig. 3B). The substantial

Table 1
Comparison of the analytical performance of several existing biosensors and present biosensor.

Detection system	LOD (M)	Dynamic range (M)	Reference
Impedimetric	**2.3×10^{-14}**	**1.0×10^{-13}–1.0×10^{-10}**	Gong et al. (2016)
Impedimetric	**3.0×10^{-13}**	**1.0×10^{-12}–1.0×10^{-9}**	Gong et al. (2015)
ECL	**22×10^{-15}**	**1.0×10^{-13}–1.0×10^{-10}**	Ruan et al. (2014)
Electrochemical	**7.05×10^{-12}**	–	Guo et al. (2013)
Electrochemical	**1.0×10^{-10}**	**2.0×10^{-8}–1.0×10^{-7}**	Zhang et al. (2010)
Fluorescence	**4.0×10^{-10}**	**1.0×10^{-9}–5.0×10^{-8}**	Ye et al. (2016)
Impedimetric	**2.3×10^{-14}**	**1.0×10^{-13}–1.0×10^{-10}**	Gong et al. (2016)
FRET(AuNPs quencher)	**15×10^{-15}**	**50×10^{-15}–1.0×10^{-9}**	**This work**
FRET(AuNPs/GO quencher)	**5.0×10^{-15}**	**50×10^{-15}–0.4×10^{-9}**	**This work**

improvement in sensitivity of this assay by using AuNPs/GO is mainly attributed to the low background signal induced by GO. As shown in Fig. 3A, the PL peak centered at 461 nm is related to the CDs emission, this PL peak intensity at 461 nm increased when the target cDNA sequence concentration increased from 50 fM to 1.0 nM with an obvious red-shift, indicating that the aggregated dsDNA-CD-AuNPs or dsDNA-CD-AuNPs-GO separated to dsDNA-CD, AuNPs and AuNPs-GO. Inset in Fig. 3A is the digital picture of capture probe ssDNA-CDs (the a labeled vials), capture probe ssDNA-CDs/AuNPs (the b labeled vials) in the presence of target DNA sequence with different concentrations (the c labeled vials), suggesting the obvious color changes induced by target DNA sequence. In Fig. 3B and D the results related to AuNPs/GO is presented. The regression equation was written in related graphs (C is in units of pM). As illustrated, the fluorescence response increased linearly with increasing target DNA concentrations in three concentration range, between 0.05–0.75 pM, 0.75–80 pM and 80–1000 pM for AuNPs as quencher and 0.05–1.0 pM, 2.0–10 pM and 10-400 pM for AuNPs/GO as quencher, respectively. The detection limit of 15 fM obtained from an ssDNA-CD-AuNPs complex and the 5 fM obtained from a ssDNA-CD-AuNPs/GO assembly. As shown in Fig. 3B, with increasing the concentration of target DNA, the fluorescence response dramatically increased, implying the increase of the amount of dsDNA. Furthermore, the fluorescence recovered signals showed a clear linear dependence on the target DNA concentration for both of designed architectures but recorded data showed a higher degree of sensitivity for AuNPs/GO as quencher compared to AuNPs in all linear ranges (Fig. 3B and D). These findings reveal that AuNPs/GO based system enables highly sensitive DNA quantification. A comparison of the analytical performance of several existing biosensors with presented work is provided in Table 1. As can be seen, the analytical characteristics of the proposed method are comparable or better than reported values in literature.

3.6. The specificity of biosensor

The histogram below shows the specificity of the proposed detection method that was evaluated using ssDNA-CD to hybridize with three kinds of DNA sequences, including complementary target DNA, two-base mismatched DNA and noncomplementary DNA at the same concentration with the procedures of complementary DNA, respectively. The results are shown in Fig. 4. It was found that two-base mismatched DNA as target change the fluorescence intensity slightly compared with that of complementary DNA. Furthermore, there was almost no change in the fluorescence intensity of noncomplementary DNA as analyte compared with complementary, indicate hybridization of the non-complementary DNA with the probe DNA not observed. In contrast, the assay system showed a dramatically higher fluorescence change at the same concentrations of cDNA. To further assess the specificity of our method, the two base mismatched sequences and complementary sequences were mixed together at different mole ratios of 1:1, 10:1 and 100:1 with a total concentration of 1 nmol L^{-1} (seen in Fig. 4B). As shown in Fig. 4B, the signal decreased sharply when the mole ratio increased from 1:1–10:1 and decreased slowly from 10:1–100:1. Obvious changes of fluorescence intensity could be observed even when the two-base mismatched sequences to complementary sequences 100:1. This result indicated that the complementary sequences could be detected in the presence of 100-fold excess two-base mismatched sequences. Furthermore, the application the method for analysis of the real samples was also evaluated. The human serum was used as real sample and recovery of different added HIV DNA target was employed. The proposed optical biosensor exhibited good sensi-

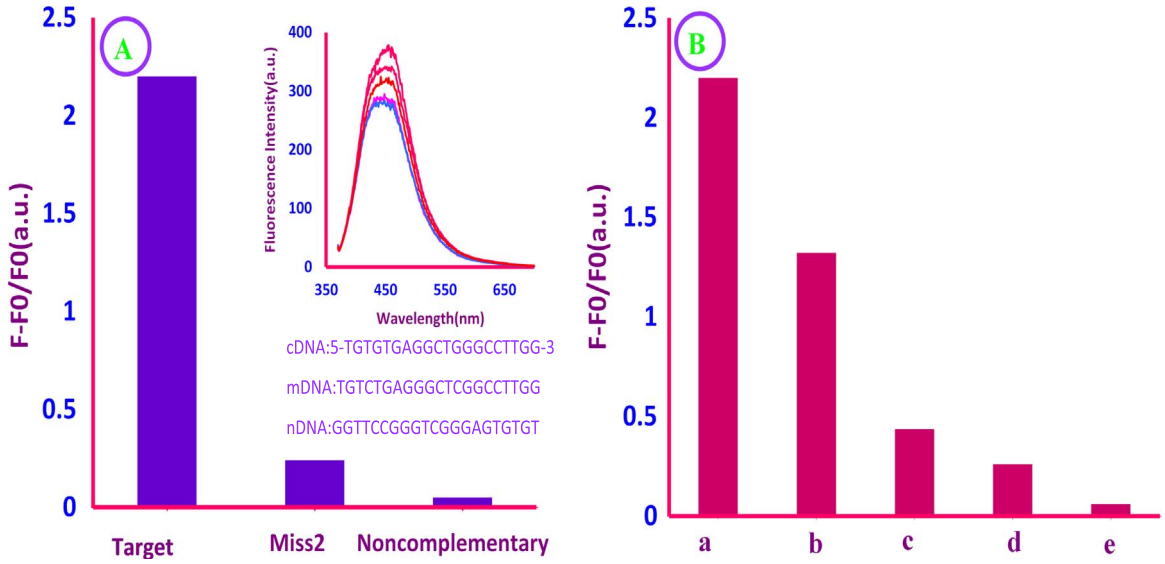

Fig. 4. (A) Histogram related to ssDNA-CDs/AuNPs conjugates after incubation with 1.0 nM of (a) target DNA (b) two-base mismatched strand, and (c) non complementary in the presence of 0.22 nM AuNP. (B) The histograms of the analytical signal of different ratios of double-base mismatched to complementary DNA: 1:1 (b), 10:1 (c), 100:1 (d); control experiments: 1.0 nmol /L complete complementary sequences (a) and 1.0 nmol/L double-base mismatched sequences (e).

tivity and high percentage recovery in real serum samples, recoveries were in the range of 95.0–98.5%, and RSDs values were in the range of 4.03–5.72% (more details is in SI file). Thus, the designed immunoassay could be effectively applied for the detection of HIV in human serum.

4. Conclusion

The excellent specificity combined with high sensitivity and fast response of the ssDNA-CDs-AuNPs/GO complex to target DNA suggests that this sensing assay might have the capacity to be applied to detecting other target DNA sequences. In conclusion, the fabricated new FRET-based DNA sensor using ssDNA functionalized CDs as the energy donor and AuNPs, AuNPs/GO as efficient quenchers, demonstrated the efficiency down to the femtomolar level. This high performance can be attributed to the synergist cooperation between CDs and AuNPs. Since this FRET sensor is based on the use of CDs in a DNA hybridization homogeneous assay, the signal contrast has been excellent and offers advantages such as the absence of light scattering and auto fluorescence. This study also demonstrates the potential of the emerging surface functionalized CDs in optical sensing. The application of the proposed assay for HIV DNA target in human serum sample has been evaluated. Therefore, our results confirmed that CDs-AuNP conjugates could be an effective tool in a FRET-based assay and could be successfully applied in the development of high sensitive and simple efficient optical sensors with great potential for clinical applications in the analysis of HIV and other DNA sequences.

Acknowledgments

The financial supports of Iranian Nanotechnology initiative and Research Office of University of Kurdistan are gratefully acknowledged.

Appendix A. Supplementary material

Supplementary data associated with this article can be found in the online version at http://dx.doi.org/10.1016/j.bios.2016.10.033.

References

Arabzadeh, A., Salimi, A., Ashrafi, M., Soltanian, S., Servati, P., 2016. Catal. Sci. Technol. 6, 3485–3496.
Bohunicky, B., Mousa, S.A., 2011. Nanotechnol. Sci. Appl. 4, 1–10.
Choi, S.O., Rezk, N.L., Kashuba, A.D., 2007. J. Pharm. Biomed. Anal. 43, 1562–1567.
Chen, N.T., Cheng, S.H., Liu, C.P., Souris, J.S., Chen, C.T., Mou, C.Y., Lo, L.W., 2012. Int. J. Mol. Sci. 13, 16598–16623.
Chikkaveeraiah, B.V., Bhirde, A.A., Morgan, N.Y., Eden, H.S., Chen, X., 2012. ACS Nano 6, 6546–6561.
Dai, H., Shi, Y., Wang, Y., Sun, Y., Hu, J., Ni, P., Li, Z., 2014. Sens. Actuator B-Chem. 202, 201–208.
Gedi, V., Kim, Y.P., 2014. Sensors 14, 18302–18327.
Gong, Q., Yang, H., Dong, Y., Zhang, W., 2015. Anal. Methods 7, 2554–2562.
Gong, Q., Wang, Y., Yang, H., 2016. Biosens. Bioelectron..
Guo, Y., Chen, J., Chen, G., 2013. Sens. Actuators B 184, 113–117.
Jafari, F., Salimi, A., Navaee, A., 2014a. Electroanalysis 26, 530–540.
Jafari, F., Salimi, A., Navaee, A., 2014b. Electroanalysis 26, 1782–1793.
Jaiswal, A., Ghosh, S.S., Chattopadhyay, A., 2012. Chem. Commun. 48, 407–409.
Lee, K.B., Kim, E.Y., Mirkin, C.A., Wolinsky, S.M., 2004. Nano Lett. 4, 1869–1872.
Lee, S.H., Bae, K.H., Kim, S.H., Lee, K.R., Park, T.G., 2008. Int. J. Pharm. 364, 94–101.
Li, X., Zhang, S., Kulinich, S.A., Liu, Y., Zeng, H., 2014. Sci. Rep. 4, 4976–4984.
Lim, S.Y., Shen, W., Gao, Z., 2015. Chem. Soc. Rev. 44, 362–381.
Muszynski, R., Seger, B., Kamat, P.V., 2008. J. Phys. Chem. C 112, 5263–5266.
Navaee, A., Salimi, A., 2013. Electrochim. Acta 105, 230–238.
Pau, C.P., Wells, S.K., Rudolph, D.L., Owen, S.M., Granade, T.C., 2010. J. Virol. Methods 164, 55–62.
Proffitt, M., 1993. Acquired immunodeficiency syndrome. Anal. Chem. 65, 396–400.
Ruan, S., Li, Z., Qi, H., Gao, Q., Zhang, C., 2014. Microchim. Acta 181, 1293–1300.
Salimi, A., Rahmatpanah, R., Hallaj, R., Roushani, M., 2013. Electrochim. Acta 95, 60–70.
Song, S., Wang, L., Li, J., Fan, C., Zhao, J., 2008. Trends Anal. Chem. 27, 108–117.
Shafiee, H., Lidstone, E.A., Jahangir, M., Inci, F., Hanhauser, E., Henrich, T.J., Kuritzkes, D.R., Cunningham, B.T., Demirci, U., 2014. Sci. Rep. 4, 4116.
Taylor, C.F., Taylor, G.R., 2004. Current and emerging techniques for diagnostic mutation detection. An overview of methods for mutation detection. Mol. Diagn. Genet. Dis. 92, 9–44.
Tothill, I.E., 2009. Sem. Cell Dev. Biol. 20, 55–62.
Tang, L., Ji, R., Cao, X., Lin, J., Jiang, H., Li, X., Teng, K.S., Luk, C.M., Zeng, S., Hao, J., Lau, S.P., 2012. ACS Nano 6, 5102–5110.
Ye, Y.D., Xia, L., Xu, D.D., Xing, X.J., Pang, D..W., Tang, H.W., 2016. Biosens. Bioelectron. 85, 837–843.
Zhang, D., Peng, Y., Qi, H., Gao, Q., Zhang, C., 2010. Biosens. Bioelectron. 25, 1088–1094.
Zhang, L., Han, Y., Zhu, J., Zhai, Y., Dong, S., 2015. Anal. Chem. 87, 2033–2036.